

Extended approximation for the lowest-lying states in odd-mass nuclei

S. Mishev* and V. V. Voronov†

Joint Institute for Nuclear Research, 6 Joliot-Curie str., Dubna 141980, Russia

(Received 2 November 2010; published 17 December 2010)

An enhanced model, based on the extended boson approximation, for the lowest-lying states in odd-mass nuclei is presented. Our approach is built on the quasiparticle phonon model, extending it to take into account the ground-state correlations due to the action of the Pauli principle more accurately than in the conventional theory. The derived interaction strengths between the quasiparticles and the phonons in this model depend on the quasiparticle occupation numbers explicitly coupling the odd-mass nucleus equations with those of the even-even core. Within this model we calculated the transition probabilities in several Te, Xe, and Ba isotopes with $A \approx 130$.

DOI: [10.1103/PhysRevC.82.064312](https://doi.org/10.1103/PhysRevC.82.064312)

PACS number(s): 21.60.Jz, 21.60.Ev

I. INTRODUCTION

Due to its simplicity and numerous successful applications the random phase approximation (RPA) [1–3] is widely considered as a good first approximation to study small fluctuations in atomic nuclei. However, this simple model enjoys only a limited success when one needs to describe properties of states from the lowest part of the spectrum in nuclei remote from the magic configurations. The quasi-boson approximation (QBA), underlying the RPA, stimulates a discussion concerning its applicability to the problem of correctly taking into account the ground state correlations (GSC) in even-even nuclei. Numerous improvements of this theory with respect to adding correlations in the ground states of even-even nuclei have been attempted, as for example in [3–7]. These enhanced models stem from the disregard of the QBA and are related to more precise inclusion of the Pauli principle when calculating matrix elements of various operators. An enhanced version of this approximation, referred to as an extended RPA (ERPA), which was proposed a long time ago [8] and later developed in [9,10], proved successful in improving the theoretical results for most measurable quantities near the nuclear ground states as, for example, the transition charge densities in the interior region.

In the present work, we follow the ERPA approach, extending it to provide a refined version of the quasiparticle phonon model (QPM) for odd-even nuclei [11–14]. The interaction strengths between the quasiparticles and phonons in the presented model depend on the number of quasiparticles in the ground state. In this way, the core-particle equations couple with the generalized equations describing the pairing correlations and the excited vibrational states of the even-even core, thus forming a large nonlinear system. This model is applicable to open-shell spherical and transitional odd- A nuclei where the Pauli principle effects are becoming essential as the number of nucleons in the unclosed shell increase.

Our research descends from the studies presented in [14,15]. There it has been shown that the backward amplitudes in the wave functions of these nuclei play a very important role for better agreement with the experimentally measured

spectroscopic factors and the properties of the states from the lower part of the energy spectrum. The theory in the latter papers is based however on the QBA, which we intend to improve by taking into account the action of the Pauli principle more precisely due to the extended boson approximation (EBA) [8].

Another widely adopted approach to study odd- A nuclei uses the interacting boson-fermion model (IBFM). The IBFM, introduced in [16] and further extended in numerous papers (e.g., [17]), differs from our approach in that the excited states of the even-even core nucleus are created by operators of a pure boson nature. In the IBFM the core-particle interaction depends on a number of free parameters which are usually fitted to match the spectrum in the odd- A nucleus. In this respect the QPM is closer to the interacting shell model where this interaction is derived from the dynamics of the constituting nucleons.

This paper first outlines the QPM and its extension based on the EBA in even-even nuclei. A comparison between the models built on the QBA and EBA is established on the basis of the reduced transition probabilities from the ground to the first 2^+ state in even-even nuclei with $A \approx 130$. In Sec. III, we give the QPM theory for odd-even nuclei, emphasizing the effect of the renormalization on the interaction vertices. Calculations on the spectroscopic factors and transition probabilities between states in some odd-even Te, Xe, and Ba nuclei, where experimental data are available, are presented in Sec. IV. Conclusions are drawn in Sec. V.

II. EVEN-EVEN NUCLEI

This section aims to mark the basic building blocks of the QPM and its EBA extension (EQPM) for one-phonon states. The notations used in the following are the same as in [10] and [14].

In EQPM one defines the quantities ρ_j , which are proportional to the quasiparticle occupation numbers in the ground state on the level j :

$$\rho_j = \frac{1}{\sqrt{2j+1}} \sum_m \langle |\alpha_{jm}^\dagger \alpha_{jm}| \rangle, \quad (1)$$

where α denotes a quasiparticle (qp),

$$\alpha_{jm} = u_j a_{jm} - (-)^{j-m} v_j a_{j-m}^\dagger. \quad (2)$$

* mishev@theor.jinr.ru

† voronov@theor.jinr.ru

The other key constituent of the theory is the phonon operators (ph) defined as

$$Q_{\lambda\mu i}^\dagger = \frac{1}{2} \sum_{jj'} [\psi_{jj'}^{\lambda i} A^\dagger(jj'; \lambda\mu) - (-1)^{\lambda-\mu} \varphi_{jj'}^{\lambda i} A(jj'; \lambda-\mu)]. \quad (3)$$

The ground state $|0\rangle$ in Eq. (1) is the vacuum state for the phonon operators: $Q_{\lambda\mu i}|0\rangle = 0$.

We study the dynamics of nuclear systems governed by the simple Hamiltonian in the form

$$H = \sum_{\tau}^{(n,p)} \left\{ \sum_{jm} (E_j - \lambda_{\tau}) a_{jm}^\dagger a_{jm} - \frac{1}{4} G_{\tau}^{(0)} : (P_0^\dagger P_0)^{\tau} : - \frac{1}{2} \sum_{\lambda\mu} \kappa^{(\lambda)} : (M_{\lambda\mu}^\dagger M_{\lambda\mu}) : \right\}. \quad (4)$$

accounting for the nuclear mean field, the pairing, and the isoscalar multipole-multipole interactions, respectively.

If the pairing vibrations are not taken into consideration then one can obtain [10] the following modified QPM equations describing the states in even-even nuclei:

$$\frac{1}{2} \sum_j (2j+1) \left\{ 1 - \frac{(1-2\rho_j)(E_j - \lambda)}{\sqrt{(E_j - \lambda)^2 + \Delta^2}} \right\} = n, \quad (5)$$

$$\frac{G}{4} \sum_j \frac{2j+1}{\sqrt{(E_j - \lambda)^2 + \Delta^2}} (1-2\rho_j) = 1, \quad (6)$$

$$\frac{\kappa_{\lambda}}{2\lambda+1} \sum_{jj'} (1-\rho_{jj'}) \frac{(f_{jj'}^{\lambda} u_{jj'}^+)^2 (\varepsilon_j + \varepsilon_{j'})}{(\varepsilon_j + \varepsilon_{j'})^2 - \omega_{\lambda i}^2} = 1, \quad (7)$$

$$\sum_{jj'} (1-\rho_{jj'}) [(\psi_{jj'}^{\lambda i})^2 - (\varphi_{jj'}^{\lambda i})^2] = 2, \quad (8)$$

$$\rho_j = \frac{1}{2} \sum_{\lambda i j'} \frac{2\lambda+1}{2j+1} (1-\rho_{jj'}) (\varphi_{jj'}^{\lambda i})^2. \quad (9)$$

The emergence of the factors $(1 - \rho_{jj'})$ takes into account the blocking effect due to the Pauli principle and requires one to solve these equations as a system of coupled equations.

The multipole-multipole interaction strengths $\kappa^{(\lambda)}$ are treated as free parameters in our study. In the numerical calculations we kept the quadrupole-quadrupole term only because it gives the dominant part of the long-range interaction for the determination of the low-lying states' properties in the nuclei of interest. One way to fix the parameter $\kappa^{(2)}$ is to have it reproduce the energy of the first 2^+ state ($\omega_{2_1^+}$). Since a one-to-one correspondence between $\omega_{2_1^+}$ and $\kappa^{(2)}$ exists, we show most of the calculated quantities as a function of $\omega_{2_1^+}$ because its values are more intuitive and closer to the experimental values than the corresponding interaction strength values.

In the following we discuss the results obtained within the EQPM for the quasiparticle and particle occupation numbers as well as for the transition probabilities in even-even nuclei.

The differences between the quasiparticle and particle occupation numbers in ^{130}Ba as a function of the first quadrupole phonon's energy within the QPM and EQPM are presented in Fig. 1. From this figure we see that the smearing of the Fermi surface increases together with the strength of the field force (and, correspondingly, ω_{2_1} decreases). In the right panel we point out that the relative difference of the particle occupation numbers calculated within the two model variants can reach up to 5%, as is the case for the proton subshell $2d_{5/2}$.

The transition probabilities in odd-even nuclei are directly linked to the transition probabilities in their corresponding even-even cores, as will be discussed in Sec. IV. We therefore perform a comparative study of the reduced transition probabilities $B(E2|g.s. \rightarrow 2_1^+)$ in several even-even nuclei within the QPM and EQPM. The transition probabilities in the EQPM are given as

$$B(E\lambda|g.s. \rightarrow \lambda_i) = \left[\frac{1}{2} \sum_{jj'} (1-\rho_{jj'}) f_{jj'}^{\lambda} u_{jj'}^+ g_{jj'}^{\lambda i} \right]^2. \quad (10)$$

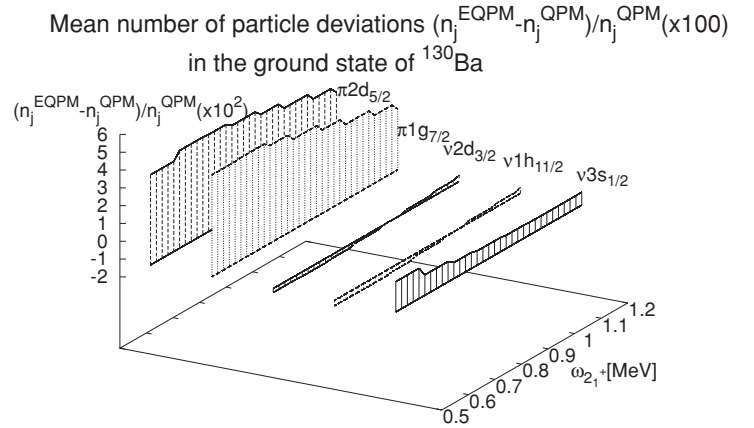
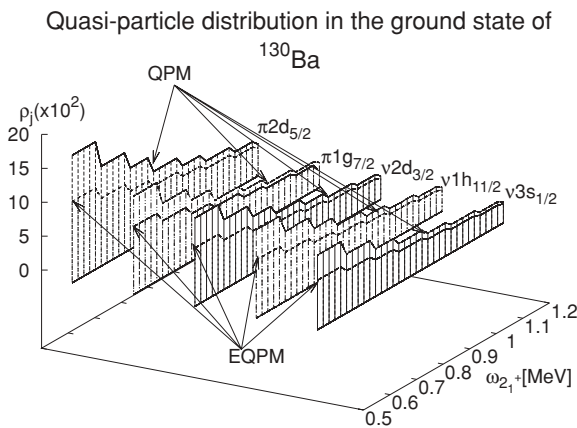


FIG. 1. Left: Quasiparticle occupation numbers $\rho_j \times 100$ in the ground state of ^{130}Ba within a one-phonon QPM and EQPM theory for the subshells in the valence shell. Right: Same as in the left panel but for the quantities $(n_j^{\text{EQPM}} - n_j^{\text{QPM}}) / n_j^{\text{QPM}} \times 100$, where n_j is the number of particles on the level j . The quantities in both panels are plotted as a function of the first quadrupole phonon's energy.

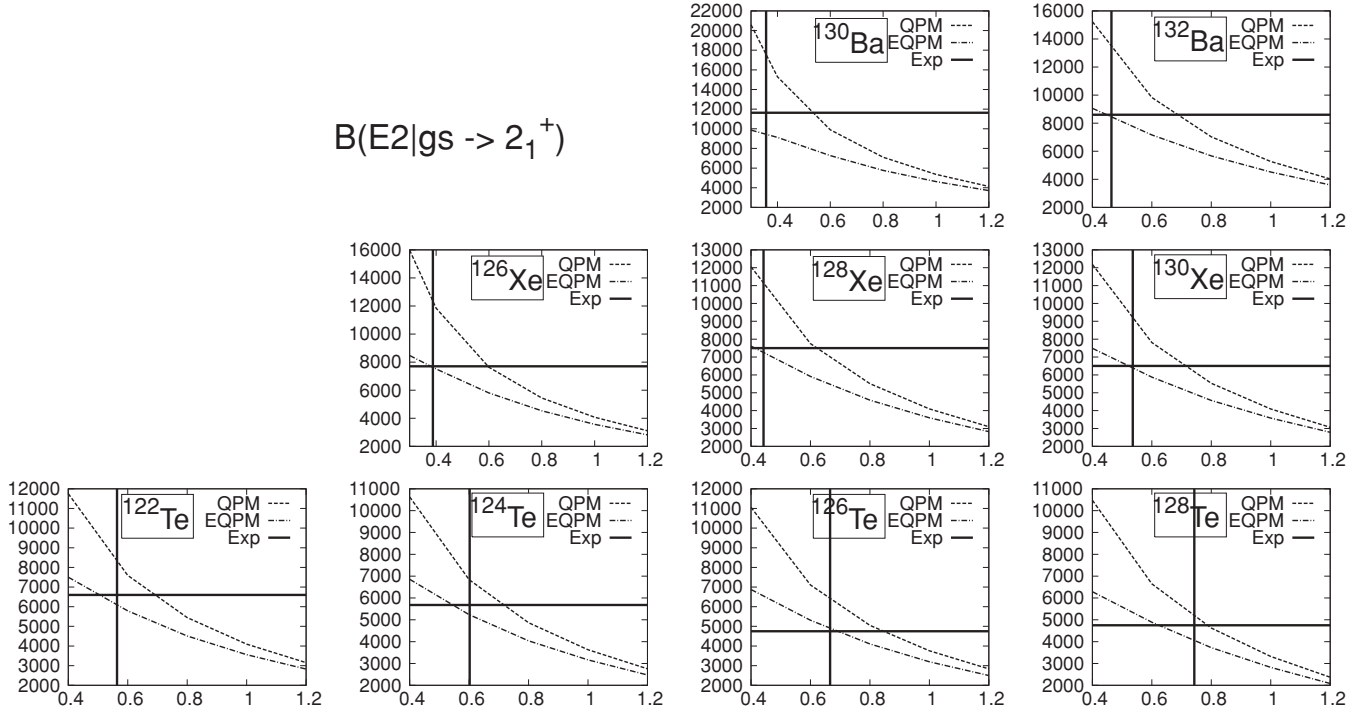


FIG. 2. The reduced transition probabilities $B(E2|g.s. \rightarrow 2_1^+)$ (in units of $e^2\text{fm}^4$) in several Te, Xe, and Ba isotopes plotted against the energy $\omega_{2_1^+}$ of the first quadrupole phonon. The solid lines represent the experimental energies and transitions.

The nuclei presented in Fig. 2 were chosen to be close to spherical ones, having $E(4_1^+)/E(2_1^+) < 2.5$. From this figure we can see that the blocking effect due to the Pauli principle exerts a large impact on this measurable quantity. The obvious superiority of the EQPM in this region serves as a motivation to study odd-even systems with a core described within the framework of this model. Besides, the transition charge densities, being related to the reduced transition probabilities, were studied in [10]. There it was shown that the application of the EQPM leads to a better reproduction of the experimentally measured distributions in the nuclear interior.

III. ODD-EVEN NUCLEI

In our treatment the states in odd-even nuclei are described as mixed states composed of pure quasiparticle and

quasiparticle \times phonon (qp \times ph) states including backward-going amplitudes [14,15]

$$\Psi_\nu(JM) = C_{J\nu}\alpha_{JM}^+ + \sum_{j\lambda i} D_{j\lambda i}(J\nu)P_{j\lambda i}^\dagger(JM) - E_{J\nu}\tilde{\alpha}_{JM} - \sum_{j\lambda i} F_{j\lambda i}(J\nu)\tilde{P}_{j\lambda i}(JM), \quad (11)$$

where $P_{j\lambda i}^\dagger(JM) = [\alpha_j^\dagger Q_{\lambda i}^\dagger]_{JM}$ is the qp \times ph creation operator and $\tilde{}$ stands for time conjugation, according to the convention $\tilde{a}_{jm} = (-1)^{j-m}a_{j-m}$.

The structure coefficients from (11) and the energies of the states in the odd- A nucleus can be obtained by making use of the equation-of-motion method. In conformance to the relation (1), when calculating the matrix elements, we obtain the following generalized eigenvalue problem:

$$\begin{pmatrix} \varepsilon_J & V(Jj'\lambda'i') & 0 & -W(Jj'\lambda'i') \\ V(Jj\lambda i) & K_J(j\lambda i|j'\lambda i') & W(Jj\lambda i) & 0 \\ 0 & W(Jj'\lambda'i') & -\varepsilon_J & -V(Jj'\lambda'i') \\ -W(Jj\lambda i) & 0 & -V(Jj\lambda i) & -K_J(j\lambda i|j'\lambda i') \end{pmatrix} \begin{pmatrix} C_{J\nu} \\ D_{j'\lambda i'}(J\nu) \\ -E_{J\nu} \\ -F_{j'\lambda i'}(J\nu) \end{pmatrix} = \eta_{J\nu} \begin{pmatrix} 1 & 0 & 0 & 0 \\ 0 & 1 - \mathcal{L}^*(Jj\lambda i) & 0 & 0 \\ 0 & 0 & 1 & 0 \\ 0 & 0 & 0 & 1 - \mathcal{L}^*(Jj\lambda i) \end{pmatrix} \begin{pmatrix} C_{J\nu} \\ D_{j'\lambda i'}(J\nu) \\ -E_{J\nu} \\ -F_{j'\lambda i'}(J\nu) \end{pmatrix} \quad (12)$$

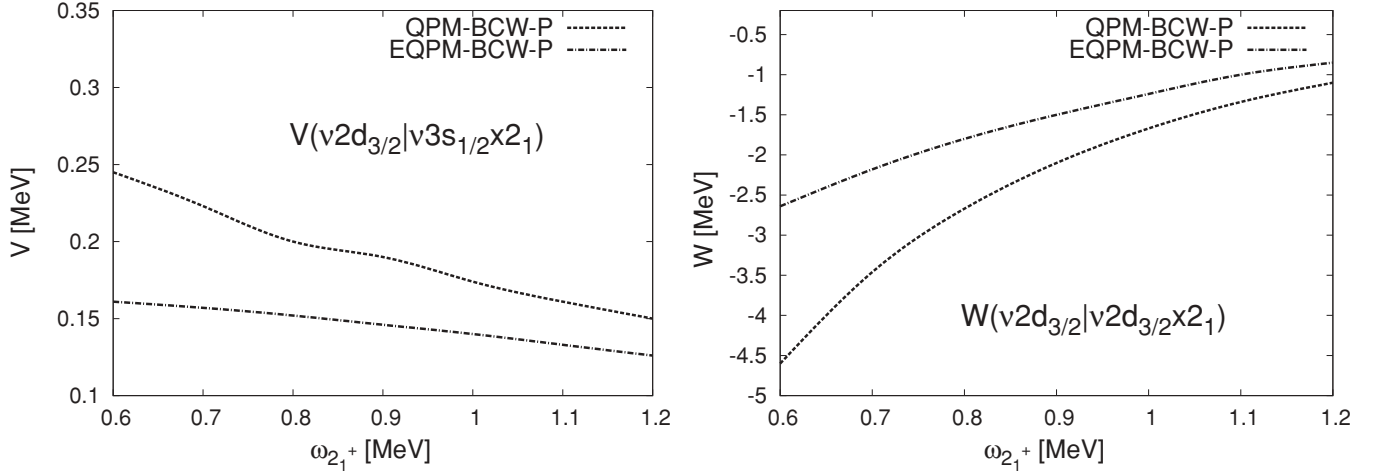


FIG. 3. The matrix elements $V(v2d_{3/2}|v3s_{1/2} \times 2_1^+)$ and $W(v2d_{3/2}|v2d_{3/2} \times 2_1^+)$ in ^{131}Ba plotted against the energy $\omega_{2_1^+}$ of the first quadrupole phonon in ^{130}Ba .

For conciseness, we provide only the leading terms of the expressions for the matrix elements:

$$\begin{aligned} V(Jj\lambda i) &= \langle \{[\alpha_{JM}, H], P_{j\lambda i}^\dagger\} \rangle \\ &= -\frac{1}{\sqrt{2}}[1 - \rho_j + \mathcal{L}^*(Jj\lambda i)]\Gamma(Jj\lambda i), \end{aligned} \quad (13)$$

$$\begin{aligned} W(Jj\lambda i) &= \langle \{[\alpha_{JM}^\dagger, H], \tilde{P}_{j\lambda i}^\dagger\} \rangle \\ &= \frac{\pi_\lambda}{\pi_J} \varepsilon_J \rho_j \varphi_{JJ}^{\lambda i} - \frac{1}{4}[1 - \rho_j + \mathcal{L}^*(Jj\lambda i)] \frac{\pi_\lambda}{\pi_J} \\ &\quad \times \sum_{i_1} \mathcal{A}(\lambda i_1 i) \varphi_{JJ}^{\lambda i_1}, \end{aligned} \quad (14)$$

$$\begin{aligned} K_J(j\lambda i | j'\lambda' i') &= \frac{1}{2}[I_J(j\lambda i | j'\lambda' i') + I_J(j'\lambda' i' | j\lambda i)] \\ &= \delta_{jj'} \delta_{\lambda\lambda'} \delta_{ii'} [1 - \rho_j + \mathcal{L}^*(Jj\lambda i)] (\varepsilon_j + w_{\lambda i}) \\ &\quad - \delta_{jj'} \delta_{\lambda\lambda'} \delta_{ii'} (1 + \mathcal{L}(Jj\lambda i)) \\ &\quad \times \frac{1}{4} \sum_{i_1} \mathcal{A}(\lambda i i_1) \mathcal{L}_{JJ}^*(j\lambda i | j\lambda i_1). \end{aligned} \quad (15)$$

For the numerical calculations we used a diagonal approximation for \mathcal{L} [12]. In the following we list the notations entering into the matrix elements (13)–(15):

$$I_J(j\lambda i | j'\lambda' i') = \langle \{P_{j\lambda i}(JM), [H, P_{j'\lambda' i'}^\dagger(JM)]\} \rangle, \quad (16)$$

$$\mathcal{L}_{JJ'}^*(j\lambda i | j'\lambda' i') = \pi_{\lambda\lambda'} \sum_{j_1} (1 - \rho_{j_1 j'}) \psi_{j_1 j}^{\lambda' i'} \psi_{j_1 j'}^{\lambda i} \begin{Bmatrix} j' & j_1 & \lambda \\ j & J & \lambda' \end{Bmatrix}, \quad (17)$$

$$\mathcal{L}^*(Jj\lambda i) = \pi_{\lambda\lambda} \sum_{j_1} (1 - \rho_{j_1 j'}) \psi_{1j}^{\lambda i} \psi_{1j}^{\lambda i} \begin{Bmatrix} j & j_1 & \lambda \\ j & J & \lambda \end{Bmatrix}, \quad (18)$$

$$A(\lambda i i') = \sum_{\tau} \frac{X_{\lambda i}(\tau) + X_{\lambda i'}(\tau)}{\sqrt{\mathcal{Y}_{\lambda i}(\tau) \mathcal{Y}_{\lambda i'}(\tau)}}, \quad (19)$$

$$X_{\lambda i}(\tau) = \sum_{jj'} \frac{(1 - \rho_{jj'}) (f_{jj'}^{\lambda} u_{jj'}^+)^2 \varepsilon_{jj'}}{\varepsilon_{jj'}^2 - \omega_{\lambda i}^2}, \quad (20)$$

$$\mathcal{Y}_{\lambda i}(p) = \mathcal{Y}_{\lambda i}(n) = \omega_{\lambda i} \sum_{jj'} \frac{(1 - \rho_{jj'}) (f_{jj'}^{\lambda} u_{jj'}^+)^2 \varepsilon_{jj'}}{(\varepsilon_{jj'}^2 - \omega_{\lambda i}^2)^2}. \quad (21)$$

In the limiting case $\rho_j = 0$, the problem in (12) is brought to the model obtained in [14]. In the following we discuss the effect of the correlations in the nuclear ground state on the behavior of the matrix elements in (12).

The interaction between the quasiparticles and the phonons will naturally become stronger when the smearing around the Fermi level increases. In Fig. 3, the dependence of sample qp-ph interaction strengths on $\omega_{2_1^+}$ is plotted. The weakening of this interaction within the extended model, as compared to the interaction derived within the QBA, is getting more salient as the ground-state correlations increase. It is also worth noting that the strengths in the backward direction depend not only on the structure of the phonon state $|\lambda i\rangle$ building the matrix element $W(Jj\lambda i)$ but also on all other phonons entering into the sum in the second summand of the right-hand side of Eq. (14). This implies that the higher-lying phonon states influence the properties of the states near the ground state. We estimated that the contribution of the higher-lying phonons to the quantities $W(Jj\lambda i)$ can be up to 25%. The diagonal matrix elements $K_J(j\lambda i | j'\lambda' i')$ exhibit a similar effect due to the second summand of the right-hand side of (14). This sum generates an energy shift, which can contribute to the appearance of intruder states in the lower part of the energy spectrum, as discussed in detail in [12].

In our previous paper [14], it was found out that the decrease in the energy of the first 2_1^+ state leads to a considerable growth of the quantities $W(Jj\lambda i)$, thus pushing the first solution very close to the first qp \times ph pole. This did not allow us to correctly reproduce both the properties of the odd-even nucleus and its even-even core using the same values for the multipole constants κ_λ and correspondingly $\omega_{\lambda\pi}$. We noticed that the

values of $\omega_{2_1^+}$ in the even-even core, which let us reproduce the energies of the lowest part of the spectrum in the odd-even nucleus with reasonable accuracy, were much higher than their experimental counterparts. In this regard the weakened interaction between the pure qp and $qp \times ph$ configurations (13) and (14) caused by the quasiparticle blocking should yield better agreement between the theory and the experiment.

IV. NUMERICAL RESULTS

In this section, we present numerical results showing the influence of the backward propagating terms on the spectroscopic factors and the transition probabilities between states in odd-even nuclei using the two approximations—QBA and EBA—giving rise to different variants of the model. The latter are denoted in a similar way as in [14]:

QPM_P: one-phonon model, including Pauli principle corrections (as in [12]);

QPM_BCK_P: one-phonon model, including backward amplitudes and Pauli principle corrections (as in [14]);

EQPM_BCK_P: one-phonon model, including both backward amplitudes and Pauli principle corrections having a core described within the EQPM.

In the following we give technical details on the calculations performed.

For simplicity, we employed a Wood-Saxon mean field with parameters fitted to reproduce the nuclear binding energies. In a similar way, the pairing strengths G_τ were obtained to match the odd-even mass differences in neighboring nuclei (for details see [14]). We included quadrupole phonons only since the quadrupole-quadrupole interaction, along with the pairing interaction, plays a dominant role for the low-lying collective states in even-even nuclei, as already pointed out in Sec. II. We let the quadrupole strength $\kappa^{(2)}$, correspondingly $\omega_{2_1^+}$, vary and analyze the dependence of the quantities of interest on $\omega_{2_1^+}$. The phonons' energy cutoff is set to 15 MeV. One appealing feature of the QPM and in particular of the variant described in this paper is that the interaction strengths between the quasiparticles and phonons depend only on the parameters describing their internal structure, thereby introducing no extra degrees of freedom.

From the computational perspective solving the algebraic system (5)–(9) is a more challenging task than solving the equations of the standard QPM. As an initial approximation to the solution of the coupled problem we take the solutions obtained from the uncoupled equations (i.e., $\rho_j = 0$).

We tested the so-developed approximation on several odd-*A* Te, Xe, and Ba isotopes entering into the transitional region. As has already been pointed out in Sec. II, where we investigated the properties of the corresponding even-even cores, the use of the EQPM improves the agreement between the results of the calculations and the experimental data significantly.

First, we head off to investigate the single-particle components of the wave function. In the model versions which take into account the backward amplitudes we found a serious depletion of the quasiparticle strengths as exemplified in Fig. 4 for the case of the qp state $\nu 2d_{5/2}$. We found a similar behavior for the rest of the states from the valence shell in all nuclei

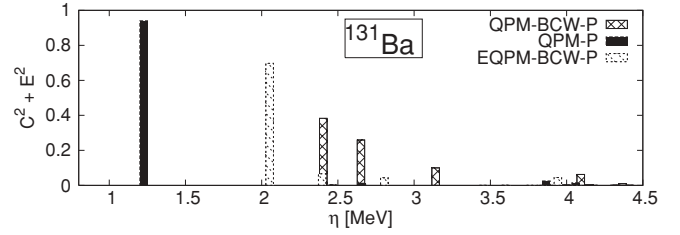


FIG. 4. Quasiparticle strength distribution ($C^2 + E^2$) of the state $\nu 2d_{5/2}$ in ^{131}Ba . The quadrupole-quadrupole interaction strength $\kappa^{(2)}$ is kept constant in the calculations within the three model versions.

within the considered region. An appropriate experimentally measurable quantity to study the single particle strength is the spectroscopic factor (SF) for the (d, p) reaction, calculated as

$$S_{J\nu} = (C_{J\nu} u_J - E_{J\nu} v_J)^2. \quad (22)$$

From Fig. 5 we see that the value of $\omega_{2_1^+}$, at which the experimentally measured spectroscopic factor is reproduced, is lower in the case of EQPM_BCK_P than in QPM_BCK_P by about 50 keV and is therefore closer to the energy of the first 2^+ state in ^{130}Ba . In Table I, this comparison between the two model versions is extended for several nuclei where experimental data are available. From there we see a systematic improvement with respect to $\omega_{2_1^+}$ ranging from 50 to 150 keV in favor of EQPM_BCW_P.

While the spectroscopic factors are influenced mainly by the properties of the last, unpaired particle, the electric transition probabilities depend strongly on the bulk properties of the even-even core. The largest contribution to these quantities is due to transitions between pure qp and $qp \times ph$ states represented by the sum in the right-hand side of the following expression:

$$B_{\text{odd}}(E\lambda; J_1\nu_1 \rightarrow J_2\nu_2) = \frac{1}{\pi^2 J_1} \left(C_{J_1\nu_1} C_{J_2\nu_2} e_{np} f_{J_1 J_2}^\lambda v_{J_1 J_2}^- + \sum_i U(J_1\nu_1 J_2\nu_2 \lambda i) \sqrt{B(E\lambda; \text{g.s.} \rightarrow \lambda_i)} \right)^2, \quad (23)$$

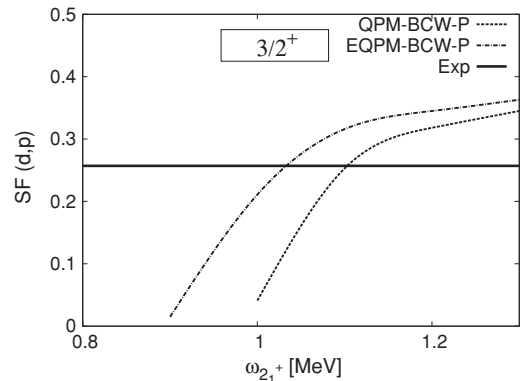


FIG. 5. Spectroscopic factor for the (d, p) reaction in ^{131}Ba as a function of $\omega_{2_1^+}$.

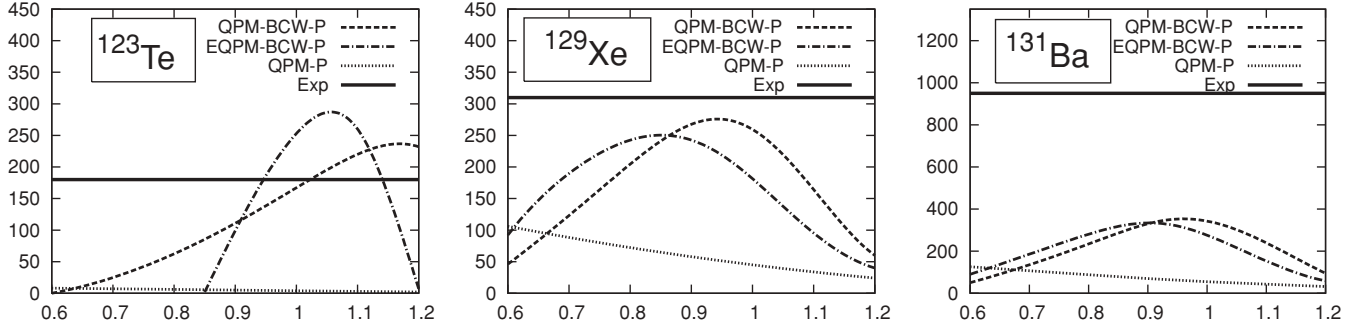


FIG. 6. Same as Fig. 5 but for $B(E2|3/2_1^+ \rightarrow 1/2_1^+)$ in ^{123}Te , ^{129}Xe , and ^{131}Ba .

where e_{np} is 1 if the unpaired particle is a proton and 0 if it is a neutron; $B(E\lambda; \text{g.s.} \rightarrow \lambda_i)$ is the reduced transition probability in the corresponding even-even nucleus given by formula (10) and

$$\begin{aligned}
 U(J_1\nu_1 J_2\nu_2 \lambda i) = & \frac{\pi J_1}{\pi_\lambda} [C_{J_2\nu_2} D_{J_2\lambda i}(J_1\nu_1) \\
 & - E_{J_2\nu_2} F_{J_2\lambda i}(J_1\nu_1)] [1 + L(J_1 J_2 \lambda i)] \\
 & + (-1)^{J_1 - J_2 + \lambda} \frac{\pi J_2}{\pi_\lambda} [C_{J_1\nu_1} D_{J_1\lambda i}(J_2\nu_2) \\
 & - E_{J_1\nu_1} F_{J_1\lambda i}(J_2\nu_2)] [1 + L(J_2 J_1 \lambda i)]. \quad (24)
 \end{aligned}$$

In expression (23) the terms corresponding to transitions between pure $qp \times ph$ states have been neglected as being small. In systems where the last particle is a neutron we make the approximation

$$\begin{aligned}
 B_{\text{odd}}(E\lambda; J_1\nu_1 \rightarrow J_2\nu_2) \\
 = \frac{1}{\pi_{J_1}^2} \left[\sum_i U(J_1\nu_1 J_2\nu_2 \lambda i) \sqrt{B(E\lambda; \text{g.s.} \rightarrow \lambda_i)} \right]^2 \\
 \approx \frac{1}{\pi_{J_1}^2} U^2(J_1\nu_1 J_2\nu_2 \lambda 1) B(E\lambda; \text{g.s.} \rightarrow \lambda_1), \quad (25)
 \end{aligned}$$

which stems from the fact that the coefficients $U(J_1\nu_1 J_2\nu_2 \lambda i)$ are non-negligible for the lowest-lying states only and out of these states the transition to the first excited state is the strongest.

The dependence $B_{\text{odd}}(E2|3/2_1^+ \rightarrow 1/2_1^+) = B_{\text{odd}}(E2|3/2_1^+ \rightarrow 1/2_1^+)(\omega_{2_1^+})$ is plotted in Fig. 6 within the three

TABLE I. Spectroscopic factors for the (d, p) reaction of the state $3/2_1^+$ in ^{123}Te , ^{125}Te , ^{127}Te , and ^{131}Ba . The second column gives the experimental [18] values (Exp). The third and fourth columns give the energies $\omega_{2_1^+}$ (in MeV) of the corresponding even-even cores calculated within QPM and EQPM at which the experimental values of the SF are reproduced.

Nuclide	Exp	$\omega_{2_1^+}$, QPM_BCW_P	$\omega_{2_1^+}$, EQPM_BCW_P
^{123}Te	0.5	1.4	1.3
^{125}Te	0.46	1.5	1.3
^{127}Te	0.38	1.5	1.35
^{131}Ba	0.25	1.05	1

model versions. This function shows an almost linear behavior in the case of the QPM_P while in the calculations which take into account the backward amplitudes a peak emerges. This peak is a result of the increased fragmentation in the latter pair of model versions (cf. Fig. 4), which contributes to the enhanced values of the coefficients $U(J_1\nu_1 J_2\nu_2 \lambda i)$. As a result, the maximum value of the presented transition probabilities in the EQPM_BCW_P and QPM_BCW_P is about three times as large as the maximum value obtained within the QPM_P, bringing us closer to the experimental values. It is also worth noting that the values of $\omega_{2_1^+}$, which correspond to the peak values obtained within the EQPM_BCW_P, are about 100 keV lower than in the QPM_BCW_P. We therefore conclude that the effect of the renormalization yields better results with respect to the experimentally measured energy of the corresponding even-even core though it is still rather higher from it.

V. SUMMARY AND OUTLOOK

In this work we extended the model presented in [14] by taking into account the blocking effect due to the Pauli principle, following the approach prescribed in [8] and [10]. Renormalized quasiparticle-phonon interaction strengths in both the forward and backward directions have been derived. Numerical calculations on the spectroscopic factors and transition probabilities in several Te, Xe, and Ba isotopes have been performed using a Wood-Saxon potential well and residual interaction of a pairing+quadrupole type. The results indicate an overall improved description of these experimentally measured quantities due to the weakened quasiparticle-phonon interaction strengths.

However, despite the adoption of this elaborate approximation, further improvements of the theory toward weakening of the qp - ph interaction could resolve some of the existing discrepancies with the experiment. Some steps in this direction would be the inclusion of higher multipolarities, the use of multiphonon configurations, and the development of a more elaborate approach to account for further correlation effects. We finally conclude that our understanding of the properties of the lowest-lying states in relatively stable odd- A nuclei still lacks the desired accuracy [19].

- [1] D. J. Thouless, *Nucl. Phys.* **22**, 78 (1961).
- [2] G. E. Brown, J. A. Evans, and D. J. Thouless, *Nucl. Phys.* **24**, 1 (1961).
- [3] D. J. Rowe, *Phys. Rev.* **175**, 1283 (1968).
- [4] H. Lenske and J. Wambach, *Phys. Lett. B* **249**, 377 (1990).
- [5] F. Catara *et al.*, *Nucl. Phys. A* **579**, 1 (1994).
- [6] J. D. Providencia, *Nucl. Phys. A* **108**, 589 (1968).
- [7] J. Dukelsky and P. Schuck, *Phys. Lett. B* **387**, 233 (1996).
- [8] K. Hara, *Prog. Theor. Phys.* **32**, 88 (1964).
- [9] R. V. Jolos and W. Rybarska, *Z. Phys. A* **296**, 73 (1980).
- [10] D. Karadjov, V. V. Voronov, and F. Catara, *Phys. Lett. B* **306**, 197 (1993).
- [11] V. G. Soloviev, *Theory of Atomic Nuclei* (Energoizdat, Moscow, 1989; Institute of Physics, Bristol, 1992); *Theory of Atomic Nuclei: Quasiparticles and Phonons* (Institute of Physics, Bristol and Philadelphia, 1992).
- [12] C. Z. Khuong, V. G. Soloviev, and V. V. Voronov, *J. Phys. G* **7**, 151 (1981).
- [13] A. I. Vdovin, V. V. Voronov, V. G. Soloviev, and Ch. Stoyanov, *Part. Nucl.* **16**, 245 (1985).
- [14] S. Mishev and V. V. Voronov, *Phys. Rev. C* **78**, 024310 (2008).
- [15] V. Van der Sluys, D. Van Neck, M. Waroquier, and J. Ryckebusch, *Nucl. Phys. A* **551**, 210 (1993).
- [16] F. Iachello and O. Scholten, *Phys. Rev. Lett.* **43**, 679 (1979).
- [17] C. E. Alonso, J. M. Arias, R. Bijker, and F. Iachello, *Phys. Lett. B* **144**, 141 (1984); C. E. Alonso, J. M. Arias, and M. Lozano, *J. Phys. G* **13**, 1269 (1987).
- [18] [<http://www.nndc.bnl.gov/ensdf/>].
- [19] P. F. Bortignon *et al.*, *J. Phys. G* **37**, 064013 (2010).